Design, implementation, and preliminary in-vivo assessment of a high-CMRR low-NEF wireless EEG miniaturized platform

Alvaro Ríos[1], Gonzalo Gutiérrez[1], Carolina Cabrera[1], Pedro Aguilera[2], Ángel Caputi[2] and Julián Oreggioni[1]

***Abstract*— This work presents the design, manufacture, test, and preliminary in-vivo assessment of the proof-of-concept of a miniaturized wireless platform for acquiring electroencephalography signals, where the input stage is a high-CMRR current-efficiency custom-made integrated neural preamplifier.**

***Clinical relevance*— Small, low-power consumption, wireless, wearable devices for chronically monitoring EEG recordings may contribute to the diagnosis of transient neurological events, the characterization and potential forecasting of epileptic seizures, and provide signals for controlling prosthetic and aid devices.**

I. Introduction

Wireless EEG (electroencephalography) is a technology that allows for the non-invasive measurement of brain activity. This technology has become increasingly important in recent years as it allows for more convenient, comfortable, and mobile measurement of brain activity [1]. Wireless EEG is helpful in research and clinical settings, where traditional EEG systems can be cumbersome and restrictive [2]. Additionally, wireless EEG can expand the use of EEG beyond the traditional laboratory setting, making it possible to study brain activity in real-world environments. The development and use of wireless EEG technology can significantly advance our understanding of the brain and its functions [3]. In recent years, there has been a growing interest in the development of miniaturized devices, which, despite having few channels (less than four), can generate relevant information [4], [5], [6].

This paper presents the proof-of-concept of a miniaturized wireless platform for acquiring EEG signals. The required bandwidth in Hz is [0.1 300], and the peak-to-peak input signal's amplitudes in μV are [10 1000]. These amplitudes need an analog-to-digital converter of at least 12 bits and a programmable gain between 60 dB and 100 dB. On the other hand, the platform has to support up to eight channels. Then, Bluetooth Low Energy (BLE) is used to handle a sampling rate of 1 ksps, enabling data transmissions of 128 kbps. The platform must be portable by small animals; therefore, the targeted size is 6.25 cm^3 (25 mm x 25 mm x 10 mm), including PCB, batteries, and all components. Likewise, the ideal autonomy is 12 hours, and a minimum of 2 hours is acceptable.

The experimental procedures involving animals described in this paper were approved by the Ethics Committee of the Instituto de Investigaciones Biológicas Clemente Estable (IIBCE), Uruguay.

This work was partially funded by CSIC (Comisión Sectorial de Investigación Científica, Uruguay), ANII (Agencia Nacional de Investigación e Innovación, Uruguay) and CAP (Comisión Académica de Posgrado).

[1]Instituto de Ingeniería Eléctrica. Universidad de la República, Montevideo, Uruguay. E-Mail: juliano@fing.edu.uy

[2]Instituto de Investigaciones Biológicas Clemente Estable, Uruguay

II. Proposed solution

A. Hardware

The platform comprises an analog front-end (AFE) and the Raytac MDBT42-512KV2 module (see Fig. 1), which includes the Nordic Semiconductors NRF52832 System on Chip (SoC).

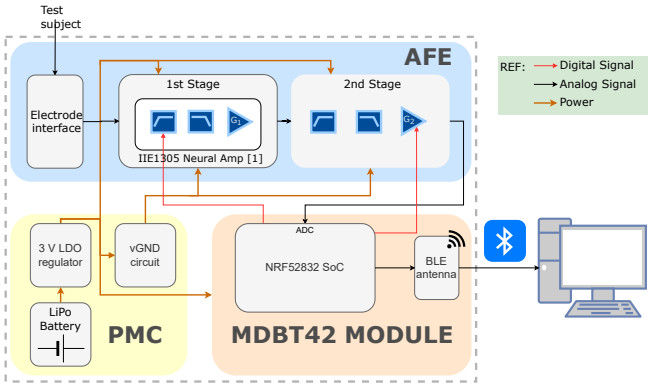

Fig. 1. Block diagram.

The AFE has two stages. The input stage is based on a custom-made high CMRR (Common-Mode Rejection Ratio) and current-efficiency (low NEF) neural preamplifier developed in [7], [8] (G1 = 50 dB). The second stage is an additional stage of filtering and gain (G2), including the LT6011 operational amplifier and the MCP4012 digital potentiometer (R_{POT}) commanded by the SoC through an up-and-down protocol, allowing the configuration of the gain G2.

The SoC occupies 8.8 mm x 13.8 mm x 1.8 mm and includes a 64 MHz ARM Cortex M4 microcontroller with 64 kB of RAM and 512 kB of FLASH, including a floating point unit, allowing on-chip advanced signal processing. In addition, the SoC/module includes eight analog inputs (12 bits), a BLE radio, and an integrated antenna.

The SoC General Purpose Input/Outputs (GPIO) pins used are: analog inputs connected to the output of the second stage of the AFE, a digital output to command the *CF* pin of the preamplifier to set the high-pass frequency; two digital outputs to command the MCP4012 chip, the *U/D* signal (up and down) to vary the resistance of R_{POT}, and *CS*, the chip select signal.

The Power Management Circuit (PMC) consists of a 3.7 V 50 mAh 1 cm^3 Li-Po battery, a TPS717 linear regulator that generates VDD = 3.0 V, and a circuit to set a reference voltage at the midpoint of VDD (vGND).

B. Embedded software

The embedded software architecture is an event-driven state machine implemented over the real-time operating system *FreeRTOS* for the nRF5 SDK (Software Development Kit). The nRF5 SDK and its FreeRTOS port provide features such as queues, event management, BLE protocol stack (known as Softdevice), peripherals drivers, and the ability to handle multiple tasks and priorities simultaneously.

The embedded software comprises several modules organized into a hierarchical four layers structure that allows for a clear separation of responsibilities by decoupling access to functions and data (see Fig. 2).

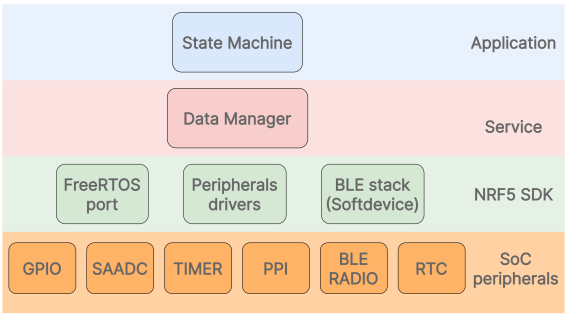

Fig. 2. Hierarchical diagram of software modules.

The highest layer is the Application layer that contains the *State Machine* module. This module implements the state machine and triggers the high-level BLE features. Below the Application layer is the Service layer, which provides the *Data Manager* module, responsible for working with the corresponding drivers to acquire samples and send them through BLE to the PC. The next layer is the nRF5 SDK layer, which implements the BLE stack (Softdevice), the FreeRTOS port, and the System on Chip (SoC) peripheral drivers used by the Data Manager and the State Machine modules. Finally, we have the SoC peripherals at the lowest layer, which provide the hardware interfaces. The following SoC peripherals are used in the platform:

- SAADC (Successive Approximation Analog-to-Digital Converter) for sample acquisition.
- GPIO (General-Purpose Input/Output) to set gain and bandwidth.
- TIMER (Timer Counter) for providing the clock for triggering the acquisition
- RTC (Real-Time Counter), used by the FreeRTOS port
- BLE radio, used by the Softdevice
- PPI (Peripheral Peripheral Interconnect) to execute actions in the ADC (Analog-to-Digital Converter) directly from the Timer peripheral events.

The state machine (see Fig. 3) has two states: *Waiting for connection (advertising)*, and *Acquisition and Transmission*.

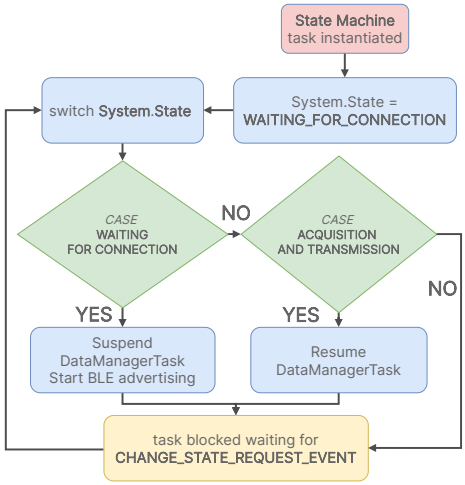

Fig. 3. Flow chart of the State Machine module.

After a power-on reset event, the platform goes to the *Waiting for connection* state. In this state, BLE Advertising is performed. BLE Advertising is a feature of the BLE standard that allows devices to broadcast messages with basic information to other devices within their range to establish a connection. The BLE Advertising is a function provided by Softdevice.

Once the connection with the PC is established, the platform enters the *Acquisition and Transmission* state. In this state, the Data Manager task is executed (see Fig. 4). During the task initialization, the ADC and the AFE are configured. The task is permanently blocked, waiting for the ADC to trigger an event when a buffer of samples is acquired. Once the samples are obtained, they are queued to the Softdevice, which sends them to the PC through BLE. Before getting blocked again, the task checks if the PC requested an adjustment of the AFE gain or bandwidth, and it adjusts if necessary.

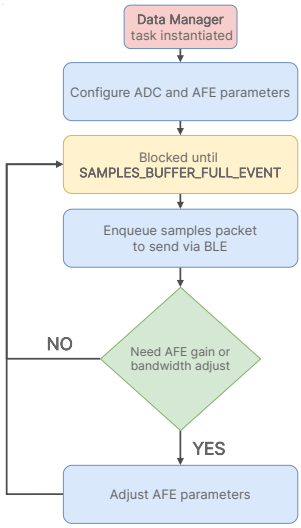

Fig. 4. Flow chart of the Data Manager module.

III. Test-bench Results

Fig. 5 shows the hardware implementation of the proof of concept of the wireless EEG platform. The platform records one EEG differential channel, its size is 20 mm x 20 mm x 10 mm, and its weight is 5.2 grams.

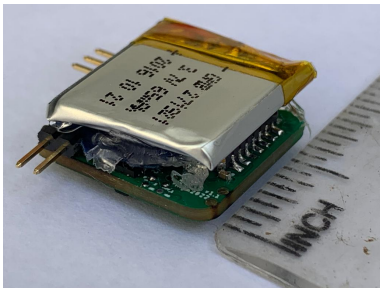

Fig. 5. Wireless EEG platform

A. Analog Front End

Fig. 6 shows the AFE frequency response. The total gain (G = G1×G2) is configurable between 63.1 dB and 100.9 dB (Fig. 7 presents the variation of G with the value of the digital potentiometer R_{POT}). At the same time, the high-pass frequency can be set between 0.1 Hz and 100 Hz. The low-pass frequency is fixed at around 350 Hz.

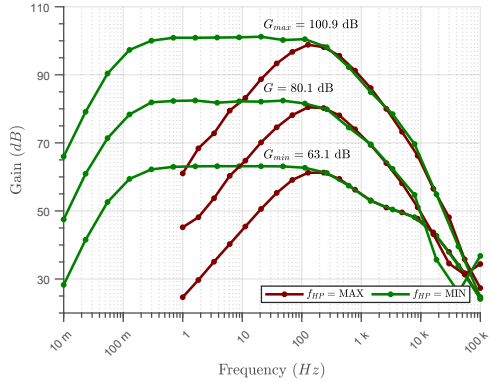

Fig. 6. AFE frequency response

Fig. 8 presents the CMRR for several values of the total gain. Fig. 9 presents the input-referred noise power spectral density. Integration under the curve divided by the gain yields an input-referred noise voltage of 0.5 μV_{rms} for the maximum gain (G = 101 dB) and 2 μV_{rms} for the minimum gain (G = 63 dB). Noise increases with the gain due to ADC quantization noise. The Noise integration bandwidth was from 10 mHz to 500 Hz.

B. Wireless data transmission

Fig. 10 shows the power spectral of a signal (a tone of 500 μV and 30 Hz) received at the PC that was sent from the platform by BLE.

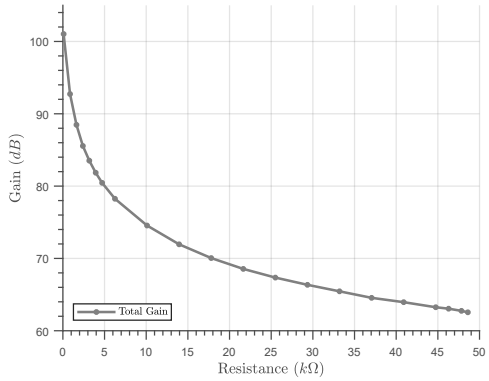

Fig. 7. AFE gain programmability.

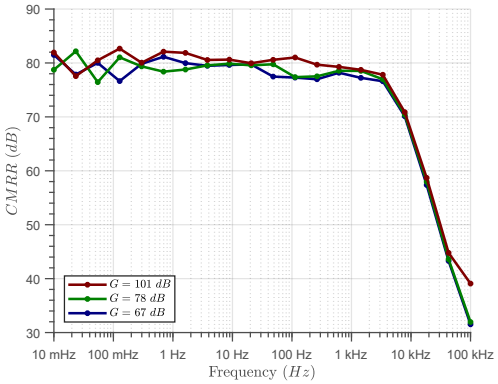

Fig. 8. Common-Mode Rejection Ratio (CMRR)

C. Current consumption and memory usage

We measured the current with Qoitech's OTII Arc when the platform operates in its main states: *waiting for connection*, and *acquisition and transmission* (see Table I). In addition, Table II shows memory usage.

TABLE I
AVERAGE CURRENT CONSUMPTION AND AUTONOMY

State	Current (mA)	Autonomy (HH:MM)
Waiting for connection	8.6	-
Acquisition and transmission	8.9	4:30

TABLE II
MEMORY USAGE

	Flash (kB)	Flash (%)	RAM (kB)	RAM (%)
Available	512	100	64	100
Used	225	43	60	94

IV. In vivo Experiments

To record EEG, we implanted a pair of twisted nichrome wires coated except at the tip at the right dorsal hippocampus (stereotaxic coordinates: bregma, -3.3, lateral, 2.7, depth, 7.0, [9]) in 2 male rats weighing 250 g, anesthetized with ketamine/xylazine (5/10 mg/Kg). These wires, and a ground

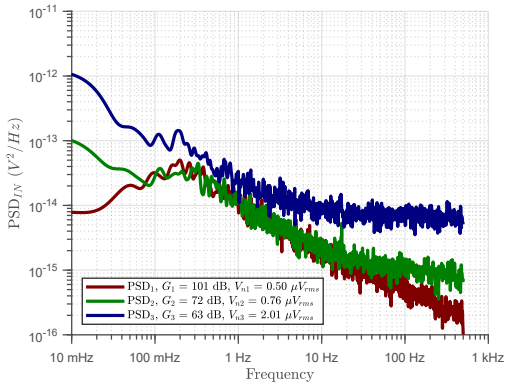

Fig. 9. Input-referred noise power spectral density

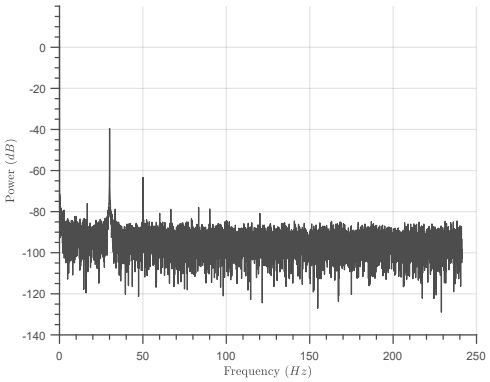

Fig. 10. Wireless transmission of a tone of 500 μV 30 Hz.

reference (a similar wire implanted subcutaneously), were previously connected to a header connector which was firmly attached to the skull using a mixture of cyanoacrylate and dental cement (Fig. 11). 48 hours later, we compared the signals recorded in the freely moving rat using our platform with those obtained using a tethered connection to an A-M Systems 1800 amplifier. We obtained similar signals with both recording devices, including theta rhythms, when the rat engaged in active motor behavior such as walking, exploratory sniffing, or gently touching (see Fig. 11).

V. Conclusions

We presented the proof-of-concept of a miniaturized BLE platform for acquiring EEG signals, where the input stage is a high-CMRR current-efficiency custom-made integrated neural preamplifier. The platform performs well in line with other state-of-the-art implementations (see Table III). The gain is configurable between 63 dB and 101 dB, and the high-pass frequency can be set between 0.1 Hz and 100 Hz. The low-pass frequency is fixed at around 350 Hz. The CMRR is 80 dB, and the input-referred noise voltage is as low as 0.5 μV_{rms}. In continuous acquisition (1 kHz) and transmission operation, the average current consumption is 8.9 mA, which allows four and a half hours of continuous operation. Preliminary in-vivo tests show the feasibility of performing recordings in small rodents.

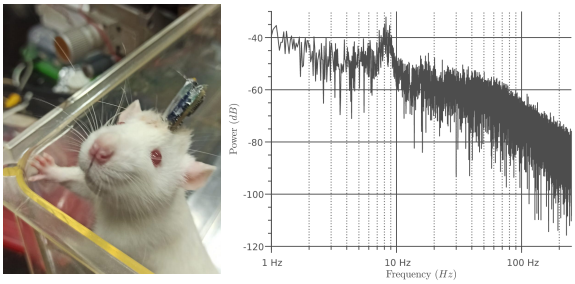

Fig. 11. In vivo recording with our platform. Right: Theta rhythms when the rat was engaged in active motor behavior.

TABLE III

Miniaturized platforms with few channels comparison.

Device	SD [5]	8274 [6]	[10]	This Work
Size LxW (mm)	25x34	32x21	45x17	20x20
Size Height (mm)	7.7	18.3	9.9	10
Weight (grams)	6.3	6.8	6.9	5.2
Channels	2	3	16	1
Data rate per ch (samples/s)	250	1024	20k	1024
Resolution (bits)	N/A	12	16	12
Comm protocol	Wired	BT	Proprietary	BLE
Noise (μV_{rms})	N/A	N/A	2.4	0.5
Bandwidth (Hz)	N/A	1 - N/A	0.1 - 5k	0.1 - 350
Gain (dB)	N/A	68	-	63 - 101
CMRR (dB)	N/A	N/A	<82	80
Autonomy (hs)	24	48	11	4.5

Acknowledgment

The authors would like to thank A. Camargo (IIBCE), F. Silveira (Fac. de Ingeniería, Udelar), and P. Braga (Sección Epilepsia, Hospital de Clínicas).

References

[1] G. Niso et al., "Wireless EEG: A survey of systems and studies," *NeuroImage*, p. 119774, 2022.

[2] V. Mihajlovic, et al, "Wearable, wireless EEG solutions in daily life applications: What are we missing?," *IEEE Journal of Biomedical and Health Informatics*, vol. 19, no. 1, pp. 6–21, Jan. 2015.

[3] A. Casson, et al, "Wearable electroencephalography," *IEEE Engineering in Medicine and Biology Magazine*, vol. 29, no. 3, pp. 44–56, 2010.

[4] L. Swinnen et al., "Accurate detection of typical absence seizures in adults and children using a two-channel electroencephalographic wearable behind the ears," *Epilepsia*, vol. 62, no. 11, pp. 2741–2752, 2021.

[5] Byteflies, "EpiCare@Home," `https://byteflies.com/`, 2020, [On line, 2023-02-12].

[6] Pinnacle Technologiy Inc, "8274 wireless system specifications," `https://www.pinnaclet.com/`, 2021, [On line, 2023-02-12].

[7] J. Oreggioni, A. A. Caputi, and F. Silveira, "Current-efficient preamplifier architecture for CMRR sensitive neural recording applications," *IEEE Transactions on Biomedical Circuits and Systems*, vol. 12, no. 3, pp. 689–699, June 2018.

[8] J. Oreggioni, P. Castro-Lisboa, and F. Silveira, "Enhanced ICMR amplifier for high CMRR biopotential recordings," in *Intl Conf of the IEEE Engineering in Medicine and Biology Society (EMBC)*, July 2019, pp. 3746–3749.

[9] G. Paxinos and C. Watson, *The rat brain in stereotaxic coordinates*, Elsevier, fourth edition, 2006.

[10] M. A. Kanchwala, G. A. McCallum, and D. M. Durand, "A miniature wireless neural recording system for chronic implantation in freely moving animals," in *2018 IEEE Biomedical Circuits and Systems Conference (BioCAS)*. IEEE, 2018, pp. 1–4.